2010 International Conference on Nanotechnology and Biosensors
IPCBEE vol.2 (2011) © (2011) IACSIT Press, Singapore

A Study on the Electrical Circuit Model for Impedance-based Microfluidic Sensor

Eun-Jung Choi, Dongil Kim, Kwang-Seok Yun
Department of Electronic Engineering,
Sogang University
Seoul, Korea
e-mail: ksyun@sogang.ac.kr

***Abstract*—In this paper, we derived the exact impedance parameter for planar electrodes system by varying configuration of electrode area, the distance between electrodes and channel width. The impedance parameters have been experimentally extracted from custom designed microfluidic chip that measures the impedance between two sensing electrodes separated by microfluidic channel. The solution resistance and electrode capacitance were fitted as 31kΩ and 0.339pF for 1mm channel length and 500 x 500 μm^2 Pt electrodes in PBS solution.**

Keywords-electrochemical impedance sensor, MEMS, microfluidic chip

I. INTRODUCTION

Building electrical impedance model associated with the interface between electrode and electrolyte is important for microfluidic sensor system. Therefore several researchers have pursued the investigation of the equivalent circuit model for the interface that consists of the electrode geometry and electrolyte parameter. The sensor based on impedance detection depends on the monitoring of electric impedance caused by the changes of conductivity and dielectric constant of the microfluidic channel.

The equivalent circuit model is used to explain the electrochemical interaction of sensors. Also the impedance data from experimental result can be analyzed and predicted by using proper electrical model.

It is reported that the coplanar electrode (both electrodes are located on the same plane) has better sensitivity comparing with the parallel plate electrodes system (both electrodes are positioned on top and bottom surfaces with facing to each other) [1]. Therefore we propose a sensor system based on measurement of the impedance using coplanar electrodes.

In this report, we construct the equivalent electrical model with various geometries of the electrodes and channels which are implemented by using micro electromechanical systems (MEMS) processes. In addition, we verify various conditions of electrodes and channel dimensions and analyze the electric circuit model by using the experimental results.

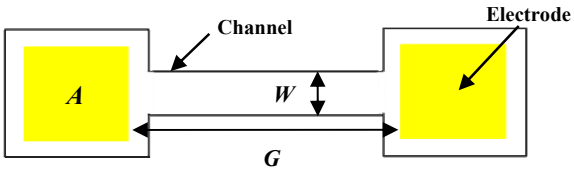

H: Channel height
W: Channel width
G: Distance between electrodes
A: Electrode area

Figure 1. The schematic of sensor with coplanar electrodes.

TABLE I. PARAMETERS AND DIMENSIONS FOR MODEL EXTRACTION.

Parameter	Dimension
Electrode area (A)	100 x 100 μm^2 300 x 300 μm^2 500 x 500 μm^2
Distance between electrodes (G)	1000 μm 500 μm 300 μm 100 μm
Channel width (W)	500 μm 300 μm 100 μm

II. DESIGN AND FABRICATION

A. Chip design

Fig. 1 shows the 2-dimensional schematic view of the proposed microfluidic chip. The chip is composed of a pair of measurement electrodes and a flow channel which forms the impedance path. In our design and experiment, the electrode area (*A*), the distance between electrodes (*G*) and the channel width (*W*) are variable parameters. The channel height (*H*) is fixed to 25 μm. Table I shows the parameters used in our experiment.

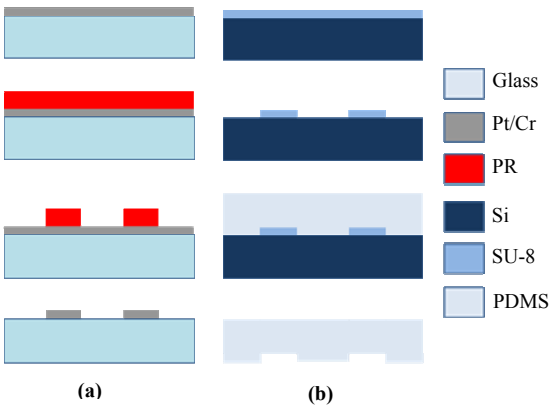

Figure 2. The fabrication process of (a) coplanar electrodes and (b) a flow channel.

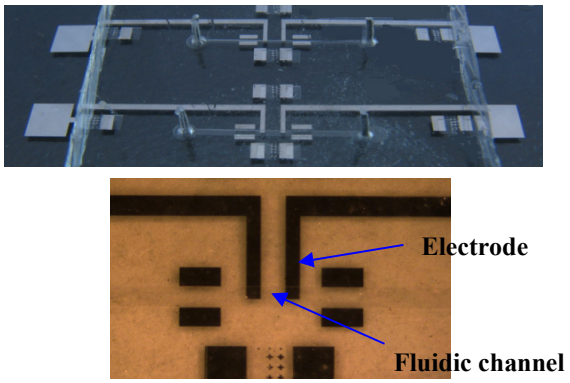

Figure 3. The fabricated chip and magnified view of the flow channel.

B. *Fabrication*

The proposed device has been implemented using a polydimethylsiloxane (PDMS) layer and a glass substrate, which are bonded together. Fig. 2 shows the fabrication procedures. For the glass substrate, the Cr/Pt (200 Å/2000 Å) layer was deposited and patterned to form electrodes after the substrate was cleaned. Then commercial wet etching solutions were used to etch the Pt and Cr films. To form the upper PDMS structures, the general PDMS replica molding method was used. First, a photosensitive epoxy, SU-8 (Microchem), is patterned on a silicon substrate to be use as a replica mold for PDMS. The SU-8 layer is coated with a thickness of 25 μm and exposed to ultraviolet (UV) light in order to define the flow channel.

The PDMS prepolymer (Dow Corning, Sylgard 184) is then poured onto the mold structure and any bubbles formed are removed in a vacuum chamber. PDMS is cured at 80 °C for 2 h and peeled gently from the substrate mold. Manual punching is used to form the access holes for the sample inlet and outlet port. Finally, the completed PDMS structure is bonded to the glass substrate following oxygen plasma treatment. Fig. 3 shows the fabricated microfluidic chip and a magnified view of the flow channel.

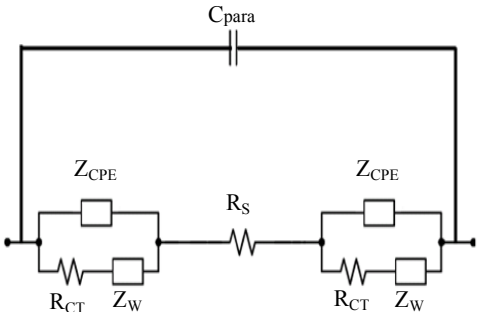

Figure 4. The equivalent circuit model for the analysis of impedance.

III. EQUIVALENT CIRCUIT

The researches for impedance spectroscopy of the interface between electrode and electrolyte have been performed and many electrical circuit models have been developed for the past years. We used the circuit model that is modified from the Randles model as shown in Fig. 4 [2, 3, 8].

In the Randles model, R_{ct} represents the charge-transfer resistance and R_s means the spreading resistance. There is diffusion of ions to the interface from the bulk of the electrolyte. This diffusion impedance or "Warburg impedance" (Z_w) is given by

$$Z_w = \frac{k}{A}\frac{\omega^{-0.5}}{1+j} \quad \cdots\cdots\cdots\cdots (1)$$

, where A is electrode area and k is a constant with unit of $\Omega \cdot s^{-0.5} \cdot cm^2$ [2, 3]. This circuit is composed of a pure resistance (R_{ct}), Warburg Impedance (Z_w) by ion diffusion, and a impedance by constant phase element (Z_{CPE}) that represents the non-ideal characteristic of double layer capacitance.

The double layer has two layers of electrical charges with opposite polarities. One charge layer is located at the metal surface and the other layer has opposite charges just inside the electrolyte. It is therefore believed that a double layer of charges exists at the solid and liquid interface which behaves much like a parallel plate capacitor.

The interface capacitance C_{dl} is the double layer capacitance. The double layer capacitance shows the characteristic of a non-ideal constant phase element (CPE), not an ideal capacitance. The following equation represents CPE [5, 6].

$$Z_{CPE} = \frac{1}{Q(j\omega)^{\alpha}} \quad \cdots\cdots\cdots\cdots (2)$$

If $\alpha = 1$, Z_{CPE} behaves as a perfect capacitance. If $\alpha = 0$, it has characteristic of a perfect resistance [2]. The resistance of electrolyte (R_s) can be expressed in the equation that consists of the electrode gap and the cross-sectional area of

channel (channel height × channel width) and the electrolyte resistivity ρ (V/m) as the parameter, which is given by

$$R_s = \rho \frac{G}{WH} \quad \cdots\cdots\cdots\cdots\cdots\cdots (3)$$

In addition, a parasitic capacitance, C_{Para}, should be considered as a parallel impedance component. This parasitic capacitance is produced by the dielectric property of the electrolyte and substrate between two electrodes.

IV. Experiemental Results

First, the flow channel was filled with Phosphate Buffered Saline (PBS, σ = 27.9mS/cm) and the electrical impedance was monitored using electrodes positioned in the channel. An LCR meter (Agilent 4284A) was used to measure the impedance at various frequencies from 100 to 100 kHz to extract measurement data for various conditions.

A. Variation of the Electrode Size

Fig. 5 shows the frequency dependency of impedance for sensors with various designs. The impedance increases at low frequency as the electrode area decreases because the relationship between Warburg impedance (Z_w) and electrode size (A) is inversely proportional to each other as shown in equation (1). And the slope at the low frequency is steeper than that of the high frequency range. In addition, the slope becomes steeper as the electrode size increases, which is well agreement with the Warburg impedance model. But the impedance at the high frequency range is almost unrelated with electrode area because capacitive components of electrolyte and double layer capacitance of the electrode surface have negligible effects on the impedance at high frequency range.

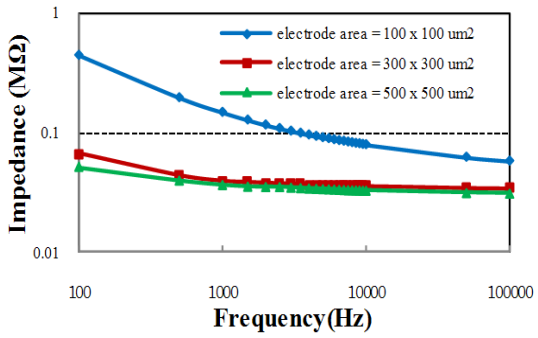

Figure 5. The magnitude of impedance according to frequency as variation of electrode area (G=1000 μm, W=500 μm).

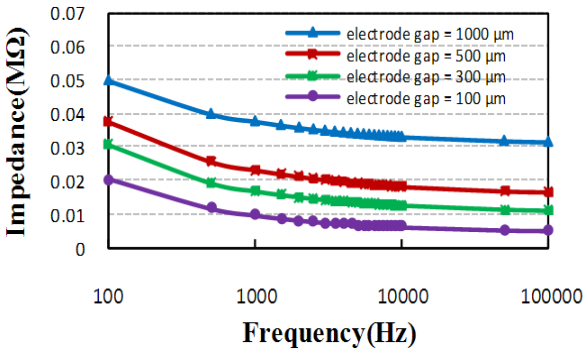

Figure 6. The magnitude of impedance according to frequency as variation of the distance of electrodes (A=500 x 500 μm^2, W=500 μm).

B. Variation of the distance between electrodes

Fig. 6 shows the impedance according to frequency changes for various distances between electrodes (G). The distances in our experiment were 1000 μm, 500 μm, 300 μm, 100 μm, respectively. The other parameters were fixed in this experiment as A is 500 x 500 μm^2 and W is 500 μm. As the distance increases, the impedance increases because the resistance of electrolyte increases. However, the slope at the low frequency is very similar with others which can be theoretically expected from equation (1) and (3).

The solution resistance (R_s) was calculated by comparing the data from the various electrode areas. Also, the electrode dimension, channel height, and the distance between electrodes, the parameters in equation (3), were used to extract the impedance data and the result was compared with the experimental result.

C. Variation of the Channel Width (W)

The magnitude of impedance was measured by using the microfluidic chips with a various channel widths (500 μm, 300 μm, 100 μm). The other parameters were fixed in this experiment (A = 100 x 100 μm^2, G = 500 μm). The resultant impedance according to the frequency is shown in Fig. 7.

As the channel width increases, the impedance decreases, which is well agreement with the result of the theoretical analysis by using equation (3). Also, the results show that there is no difference in the slope from 100 to 100 kHz even with the change of the channel width.

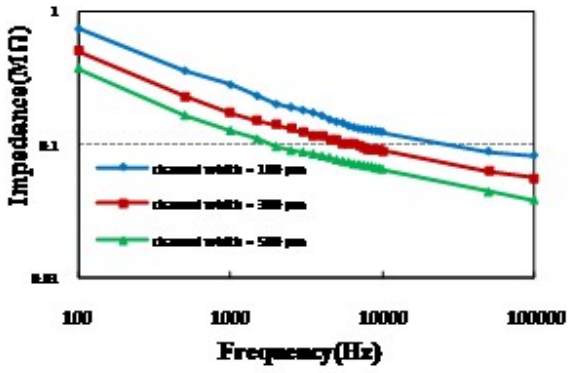

Figure 7. The magnitude of impedance according to frequency as variation of channel width (A=100 x 100 μm^2, G=500 μm)

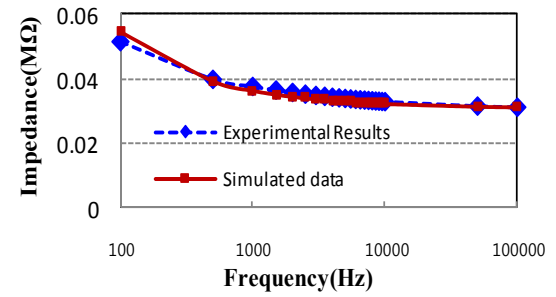

(a)

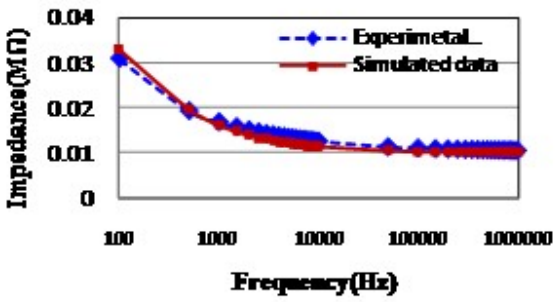

(b)

Figure 8. The experiment results and simulated data of impedance magnitude respect to the frequency. (a) A=500 x 500 μm^2, G=1000 μm, W=500 μm, (b) A=500 x 500 μm2, G=300 μm, W=500 μm.

D. Fitting between Experimental Results and Calculated Data

Fig. 8 shows the fitting results by applying the experimentally extracted data to electrical circuit model. Matlab program was used to simulate the impedance data. The parameters have been extracted from two designs; Design I having electrode area of 100 x 100 μm ^{2}, gap between two electrodes of 1000 μm and channel width of 500 μm and "Design II" having electrode area of 100 x 100 μm ^{2}, gap between two electrodes of 300 μm and channel width of 500 μm. The parameters are same for two designs except the bulk resistance because of the different channel length.

As shown in Fig. 8, the simulation results are well fitted to the experimental data. Each fitting parameters extracted from our experiments are summarized in Table II.

TABLE II. THE FITTING PARAMETERS FOR THE CIRCUIT MODEL.

Parameters	Unit	Fitting results	
		Design I	Design II
Capacitive value (Q)	[S·s $^{\alpha}$]	1.26 x 10^{-6}	1.26 x 10^{-6}
Exponent (α)		0.594791	0.594791
Charge transfer resistance (R_{ct})	[kΩ]	13.34	13.34
Solution resistance (R_s)	[kΩ]	30.99	9.3
Warburg impedance (Z_w)	[Ω·s$^{-0.5}$]	0.392 x 10^{-6}	0.392 x 10^{-6}
Parasitic capacitance (**C**)	[pF]	0.336	0.336

V. CONCLUSIONS

We have performed the impedance measurement using the coplanar electrode that has a good sensitivity. While previous works analyzed the sensors with a limited geometry, we can analyze the electrode circuit model more precisely by measuring the various geometries such as electrode area, the distance of electrodes and channel width.

The Electrode area, the gap between two coplanar electrodes and the channel width were changed as variables to analyze the frequency characteristic in impedance model. As the electrode area increased, the constant slope of the impedance magnitude decreased at low frequency range while there was little change in the solution resistance (R_s). Also the solution resistance increased as the gap between electrodes increased, while the slopes of impedance magnitude at low frequency range were not changed so much. For the channel width, the R_s increased as the channel become wide, but again the slopes of impedance magnitude at low frequency range were hardly changed. Measured data was analyzed using equivalent circuit model and the fitting parameters were found. We confirmed that the measured data well corresponded with the experimental data.

ACKNOWLEDGEMENTS

This work was supported by the National Research Foundation of Korea (NRF) grant funded by the Korea government (MEST) [331-2008-1-D00205] and research grant from Sogang University in the year 2009.

REFERENCES

[1] S. Gawad, L. Schild and P. Renaud, "Micromachined impedance spectroscopy flow cytometer for cell analysis and particle sizing", Lab on a Chip, Vol. 1, 2001, pp. 76-82.

[2] X. Huang, D. Nguyen, D.W. Greve, and M. M. Domach, "Simulation of Microelectrode Impedance Changes Due to Cell Growth", IEEE SENSORS JOURNAL, Vol. 4, Oct. 2004, pp. 576-583.

[3] E. T. McAdarns, A. Lackermeier, J. A. McLaughlin and D. Macken, "The linear and non-linear electrical properties of the electrode-electrolyte interface", Biosensors & Bioelectronics Vol. 10, 1995, pp. 67-74.

[4] Peter Van Gerwen et al., "Nanoscaled interdigitated electrode arrays for biochemical sensors", Sensors and Actuators B: Chemical, Vol. 49, 1998, pp. 73-80.

[5] C. Tlili et al, "Fibroblast Cells: A Sensing Bioelement for Glucose Detection by Impedance Spectroscopy", Analytical Chemistry, Vol. 75, 2003, pp. 3340-3344.

[6] S. Omanovic, M. MetikoS-Hukovic, “Thin oxide films on indium: impedance spectroscopy investigation of reductive decomposition”, Thin Solid Films, Vol. 266, 1995, pp. 31-37.

[7] J. Wu, Y. Ben,, D. Battigelli, and H.C. Chang, “Long-Range AC Electroosmotic Trapping and Detection of Bioparticles”, Industry & Engineering Chemistry Research, Vol. 44, 2005, pp. 2815-2822.

[8] H. Park, D. Kim, KS Yun, “Single-cell manipulation on microfluidic chip by dielectrophoretic actuation and impedance detection”, Sensors and Actuators B: Chemical Vol. 150, 2010, pp. 167-173.